The age of fossil StW573 ('Little Foot'): An alternative interpretation of ^{26}Al/^{10}Be burial data

AUTHORS:
Jan D. Kramers[1] iD
Paul H.G.M. Dirks[2]

AFFILIATIONS:
[1]Department of Geology, University of Johannesburg, Johannesburg, South Africa

[2]Department of Geosciences, College of Science and Engineering, James Cook University, Townsville, Queensland, Australia

CORRESPONDENCE TO:
Jan Kramers

EMAIL:
jkramers@uj.ac.za

Following the publication (Granger DE et al., Nature 2015;522:85–88) of an ^{26}Al/^{10}Be burial isochron age of 3.67±0.16 Ma for the sediments encasing hominin fossil StW573 ('Little Foot'), we consider data on chert samples presented in that publication to explore alternative age interpretations. ^{10}Be and ^{26}Al concentrations determined on individual chert fragments within the sediments were calculated back in time, and data from one of these fragments point to a maximum age of 2.8 Ma for the sediment package and therefore also for the fossil. An alternative hypothesis is explored, which involves re-deposition and mixing of sediment that had previously collected over time in an upper chamber, which has since been eroded. We show that it is possible for such a scenario to yield ultimately an isochron indicating an apparent age much older than the depositional age of the sediments around the fossil. A possible scenario for deposition of StW573 in Member 2 would involve the formation of an opening between the Silberberg Grotto and an upper chamber. Not only could such an opening have acted as a death trap, but it could also have disturbed the sedimentological balance in the cave, allowing unconsolidated sediment to be washed into the Silberberg Grotto. This two-staged burial model would thus allow a younger age for the fossil, consistent with the sedimentology of the deposit. This alternative age is also not in contradiction to available faunal and palaeomagnetic data.

Significance:
- Data on chert samples taken close to StW573 impose a maximum age for the fossil of 2.8 Ma – younger than the 3.67 Ma originally reported. We propose and explore a two-stage burial scenario to resolve the inconsistency and to reopen the discussion on the age of fossil StW573.

Introduction

In a recent contribution, Granger et al.[1] present ^{10}Be and ^{26}Al data on quartz from Member 2 sediments in the Silberberg Grotto in Sterkfontein Cave, South Africa, encasing StW573 ('Little Foot')[2], a complete skeleton referred to as *Australopithecus prometheus*[1]. The apparent burial isochron date of 3.67±0.16 Ma is interpreted as the age of StW573.

Almost since the discovery of StW573, its age has been a subject of controversy. Based on the concept of a laterally continuous stratigraphy for the Sterkfontein Formation[3] and a palaeomagnetic fit, an age of about 3.3 Ma was first proposed[4]. A subsequent review[5] of mainly faunal data suggested a much younger age range of between 1.5 Ma and 2.5 Ma for Member 4 at Sterkfontein as well as for the sediments encasing StW573. In a response[6], the lower age limit for Member 4 was firmly placed at ca 2 Ma (a limit since confirmed by an U-Pb age on its capping flowstone[7]) but the concerns[5] regarding an age older than 3.0 Ma for StW573 were not fully dispelled. Cosmogenic ^{26}Al/^{10}Be burial dating[8] then indicated that quartz in the sediments around the fossil had been underground for 4.17±0.35 Ma (later recalculated[1] to 3.94±0.20 Ma). Because of the possibility that the quartz was reworked from previous higher levels in the cave system, this date can be regarded as a maximum age.[1,7] In contrast, U-Pb dates[9] of ca 2.2 Ma on CaCO$_3$ speleothem units from below and above StW573 are minimum ages, as the dated units are not stratigraphic flowstones, but fracture fillings[10]. The new burial isochron date[1] fits within these age brackets.

The cave deposits encasing StW573 form the northwest flank of a sediment cone that occupies most of the Silberberg Grotto area and has its apex in the eastern part of the Grotto where the ceiling is highest.[11] The deposits consist mainly of matrix-supported breccia units composed of coarse-grained chert clasts and dolomite blocks, set in a muddy sand matrix that is mostly well calcified.[10] Stratification of the breccia units is illustrated by the presence of a finer-grained, weakly consolidated (possibly decalcified), clay-rich sand layer (Unit B2a in Bruxelles et al.[10]) near the base of the dated sedimentary pile, and variations in size (Unit B3[10]) and frequency (Unit B2b[10]) of chert and dolomite clasts, indicative of several fining upward cycles.[10] Fossil StW573 is embedded within Unit B2b and positioned along the stratigraphic top of this unit.[10] The layering, matrix-supported nature of the breccia deposits and clast size variations suggest that a succession of sheet-like, sand-rich debris flows deposited the composite package over a (geologically speaking) short period of time in a process similar to the deposition of the *A. sediba* skeletons at the Malapa site.[12] The age of the fossil must be similar to the depositional age of the breccia units as it is complete, articulated[13], and fully incorporated within the breccia.

In order to date StW573, Granger et al.[1] applied the burial isochron method[14-16] to the host breccia deposits. At the surface, quartz accumulates ^{10}Be and ^{26}Al by spallation reactions caused by neutrons, in turn produced in the atmosphere by cosmic rays. As the quartz is buried (whether in an alluvial or glaciogenic sediment, or a cave) it is shielded from neutrons and ^{10}Be and ^{26}Al production all but ceases (there is a much lower production rate at depth, caused by muons, discussed below). Because ^{26}Al decays faster than ^{10}Be, the ^{26}Al/^{10}Be abundance ratio decreases with time, allowing a burial age to be determined if their pre-burial ratio is known (this ratio can be calculated from models, or directly measured).

The data presented by Granger et al.[1] are of high quality and the interpretation appears flawless. However, the discussion on faunal data is not closed[17] and in view of the great importance of the age of StW573 in the timeline of hominin evolution, we have re-examined the data on which the 3.67 ± 0.16 Ma burial isochron date is based, and we present an alternative interpretation that is consistent with the data, but indicative of a younger age.

Chert samples, in-situ steady-state concentrations and a maximum age

In order for a burial isochron to be useful, two conditions have to be met. First, the samples must have had, at the time of burial, a primary spread in [10]Be and [26]Al concentrations that show a correlation with each other. Second, all samples must have been buried at the same time and share the same post-burial history. The cosmogenic isotopes then decay in proportion to their abundance, so that the correlation in [26]Al versus [10]Be space persists along an isochron for which the slope decreases with time.

A primary spread of [10]Be and [26]Al concentrations with a correlation can result if (1) samples are mixtures of surface derived and previously buried quartz grains[14], or (2) material with varying residence times at the surface is sampled. In the former case, a linear correlation is expected[14], whereas the latter situation results in a gentle convex-up curve[18] as a result of [26]Al decaying faster than [10]Be. In Granger et al.[1], which is the first application of burial isochron dating to cave chronology, both factors contribute to the spread of data. Six quartz separates from mainly surface-derived bulk sediment samples (ST1, ST2, ST3, ST8, ST9 and composite STM2 dark) have relatively high [10]Be and [26]Al concentrations. Further, three chert fragments (M2CA, M2CB and M2CC) taken from the breccia immediately adjacent to the fossil and a composite (STM2 light, consisting of chert grains from bulk sediment samples ST1 and ST2) have low [10]Be and [26]Al concentrations. These are considered by Granger et al.[1] to have been derived from higher levels in the cave, at a few metres below the surface. Together, these two sample populations define the slope of the isochron and thus the age. The chert samples yielded data with exquisite precision[1], and can provide more information than just the definition of an isochron by regression. To examine this aspect it is first necessary to discuss the concentration of cosmogenic nuclides produced at depth.

Cosmogenic nuclide production rates decrease rapidly with depth under the surface, as neutron penetration in soil and rock is limited to ca 2.5 m. However, even after deeper burial, quartz still accumulates cosmogenic nuclides as a consequence of the action of muons[19,20], and this subsurface nuclide production ultimately determines the concentrations of these nuclides at depth. At constant depth underground (e.g. zero erosion), the [10]Be and [26]Al concentrations of quartz derived from the surface or higher in the cave converge to in-situ steady-state or secular equilibrium (also known as saturation) values, as the abundance of each isotope is adjusted so that its loss by radioactive decay balances its production rate P (in 10^6 atoms g^{-1}Ma^{-1}), which depends on depth underground. Steady state is achieved after about 10 Ma, and the relation between P values and the in-situ concentrations (atoms g^{-1}) is then:

$$[^{10}Be]_{in\ situ} = P_{10}/\lambda_{10},\ [^{26}Al]_{in\ situ} = P_{26}/\lambda_{26} \qquad \text{Equation 1}$$

where λ_{10} and λ_{26} are the respective decay constants; $\lambda_{10}=0.4988\pm0.0050$ Ma^{-1} and $\lambda_{26}=0.9794\pm0.0230$ Ma^{-1}.[1] In the more general situation in which erosion occurs, secular equilibrium is not achieved, as the shielding by overburden is steadily reduced and the nuclide production thus increases with time. For any given present-day depth, in-situ produced cosmogenic nuclide concentrations are always lower under erosion than they would be at zero erosion.

In addition to a burial age, a [26]Al versus[10]Be isochron diagram can also yield the [26]Al and [10]Be concentrations produced in situ after burial.[1] These post-burial concentrations must plot on the isochron and also on a line through the origin of the diagram with a slope corresponding to the [26]Al/[10]Be abundance ratio of post-burial production (given by Equation 1 as ca 4.1 in steady state, although it is slightly depth dependent). This is dotted line '*s*' in Figure 1a, and its intersection with the isochron, *PI*, should represent the post-burial produced abundances: $(8.5\pm1.3)\times10^4$ atoms/g of [26]Al and $(2.1\pm0.3)\times10^4$ atoms/g of [10]Be (1σ uncertainties given, plotted with 2σ error bars).[1] We note that the uncertainty of *PI* is probably underestimated. The reason is that two of the samples analysed by Granger et al.[1] to define the isochron and the *PI* values are composites: 'STM2-light' consists of chert fragments from samples ST1 and ST2, and 'STM2-dark' of soil-derived, iron-oxide coated, rounded quartz grains from samples ST1, ST2, ST8 and ST9. The use of aggregates from multiple samples is common practice in measuring erosion rates, especially when the average value for a whole catchment is sought.[21] However, in a test for collinearity, this use is inappropriate as it hides any heterogeneity that may have existed.

The in-situ cosmogenic nuclide production rates at the StW573 site can also be calculated directly, using the equations of Heisinger et al.[19,20] and the empirically determined cross sections and probability factors reported by Balco et al.[15] The present depth below surface of StW573 is 23 m,[3,11] and the Silberberg Grotto above it was entirely filled by a flowstone boss and overlying breccia until this was mined out in the early 20th century. The bulk rock density used is 2.5 g/cm³, which (with a density of 2.85 g/cm³ for dolomite) allows for about 12% porosity if air-filled, or 8% if water-filled. An altitude correction (1500 m) was applied to the component of cosmogenic nuclides produced by stopped negative muons (accounting for between 6% and 10% of production at 23 m depth). A latitude correction, if made, would account for the deflection of cosmic rays by the earth's magnetic field at low latitudes and reduce the calculated nuclide production rates.[18,22] However, fast muons that produce the bulk of [10]Be and [26]Al at the given depth are yielded by cosmic rays with energies >20 GeV, which are unlikely to be deflected significantly. For stopped negative muons there is probably a latitude effect although it is difficult to quantify.[22] No latitude correction was applied, and the in-situ [10]Be and [26]Al concentrations obtained may be overestimated by up to a few per cent as a result.

With the above parameters, steady-state in-situ abundances of 0.0165×10^6 atoms/g [10]Be and 0.0678×10^6 atoms/g [26]Al are calculated if erosion is zero (grey diamond *calc1* in Figure 1a). If an erosion rate of 5 m/Ma (the minimum rate determined by Granger et al.[1]) is assumed, present-day in-situ abundances of 0.0120×10^6 atoms/g [10]Be and 0.0577×10^6 atoms/g [26]Al result (grey diamond *calc2* in Figure 1a). If the erosion rate was 5 m/Ma and a cave chamber had existed above the Silberberg Grotto in the past (as discussed below), calculated values would be intermediate between *calc1* and *calc2*. The higher the erosion rate, the lower the in-situ concentrations. The calculated results are, respectively, within and close to the 2σ (95% confidence) uncertainty limits of point *PI* derived from the isochron regression, which are underestimated, as discussed above. While there is thus no real contradiction between the calculated values and *PI*, the difference is nevertheless significant when reconstructing the isotope abundances of chert samples through time, as shown below.

For quartz derived from the surface or from higher levels in a cave, convergence towards the in-situ produced [10]Be and [26]Al concentrations in quartz at any depth is given by the decay law:

$$[nuclide]_t = P/\lambda + ([nuclide]_0 - P/\lambda) \times e^{-\lambda t} \qquad \text{Equation 2}$$

where $t=0$ denotes the present. Equation 2 can be used to calculate [10]Be and [26]Al concentrations in the past (with *t* being negative) and future (with *t* being positive) based on the measured concentrations at present. If erosion is non-zero, the process can be modelled by dividing it into time steps, each with its own depth-specific production rates.

As seen in Figure 1a, none of the chert samples have in-situ equilibrium [10]Be and [26]Al concentrations, in accord with the assessment[1] that they are derived from higher levels in the cave. Black arrows show their convergence on *PI* and grey arrows on *calc2*. Each sample has its own individual set of decay paths (calculated by using Equation 2 forward and backward in time from their measured concentrations), reflecting their individual histories within the cave. Further, although the concentrations of *PI* and *calc2* are not very different, the decay paths for the two points differ markedly from each other.
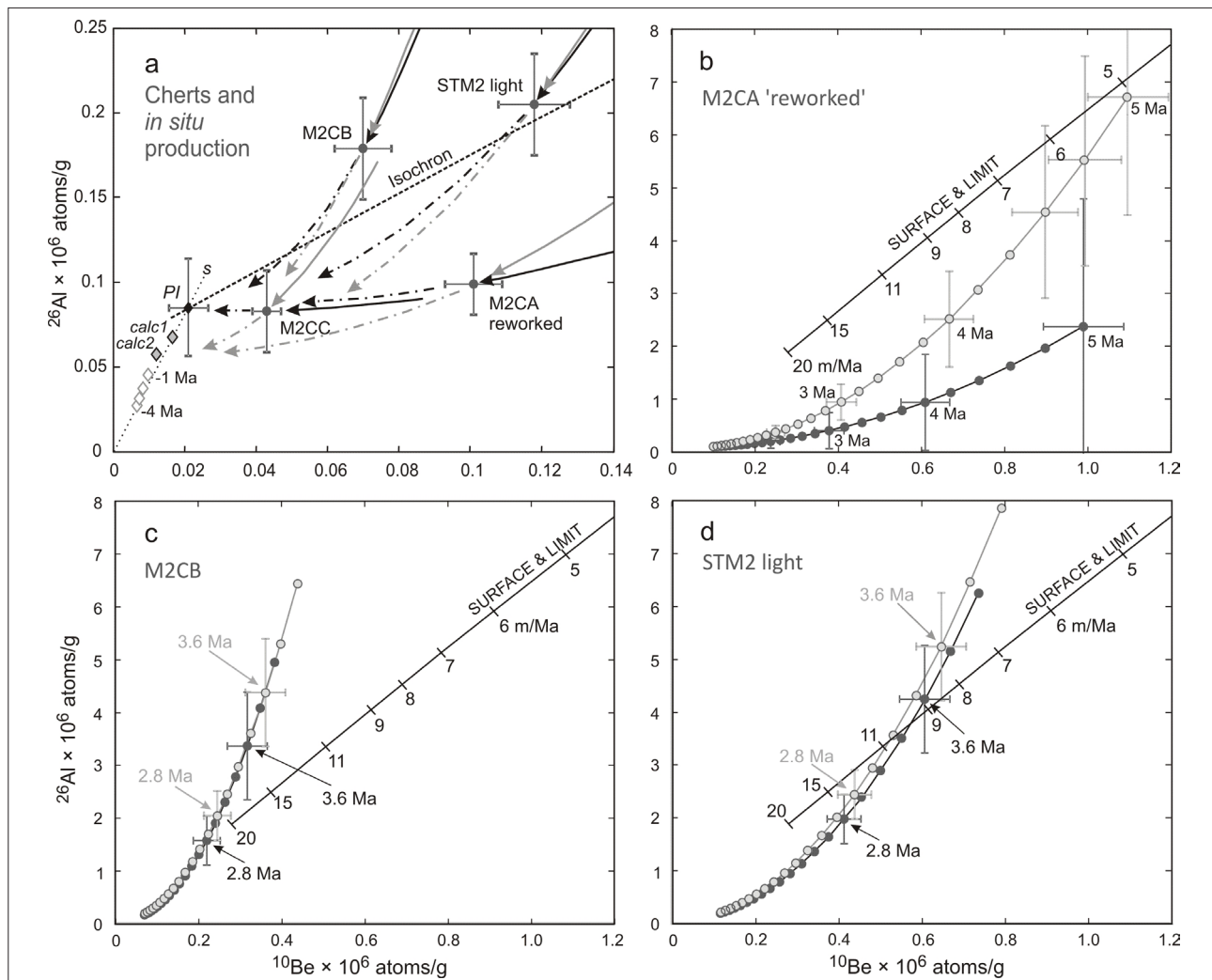
Figure 1: Chert data of Granger et al.[1] and their relationship to the in-situ produced abundances of [10]Be and [26]Al in the deposit hosting StW573. (a) Data on chert samples[1] (excluding M2CD, which plots in the 'forbidden' zone) shown with the lower part of the isochron. Post-burial in-situ produced [10]Be and [26]Al abundances must plot on or close to dotted line 's' (see text); its intersection with the isochron therefore yields the values of Granger et al.[1] (black diamond '*PI*', pivot of isochron). *PI* and all chert data shown with 2σ (95% confidence) error bars. Also shown are independently calculated in-situ abundances (grey diamonds) for a depth of 23 m and average density of 2.5 g/cm³: *calc1* shows the secular equilibrium for zero erosion and *calc2* the present day value under 5 m/Ma erosion[1], with values that quartz would have had at that location up to 4 Ma (open diamonds). The [10]Be and [26]Al concentrations of the chert samples are seen converging on in-situ points along different paths, indicating that they come from different (higher) levels in the cave system. Solid arrows depict past decay paths towards chert data as analysed, and dash–dot arrows show convergence towards the in-situ points in the future. Black arrows converge on *PI* and grey arrows on *calc2*. (b,c,d) [10]Be and [26]Al concentrations for (b) chert sample M2CA 'reworked', (c) composite chert sample MC2B and (d) chert sample STM2-light of Granger et al.[1] calculated back in time for paths corresponding to production values for *PI* (black line and symbols) and *calc* 2 (grey line and symbols). In the latter, the increase in in-situ production rates (Figure 1a) is taken into account. Error bars, shown for some ages, correspond to 2σ or 95% confidence limit. Solid line marked 'SURFACE & LIMIT' shows the steady-state abundances at the surface for erosion rates from 5 to 20 m/Ma following the surface production rates calculated by Granger et al.[1] The line also defines the upper limit for [26]Al/[10]Be ratios in quartz at or below the surface.

Sample M2CA plots significantly below the isochron, and was not included in the regression of Granger et al.[1] as it was considered reworked, i.e. to come from a previous burial location in the cave system. The back-correction for sample M2CA using production rate values for the *PI* abundances (black arrows and symbols in Figure 1b), yields a curve that lies significantly (well outside 2σ, i.e. 95% confidence) below the surface production curve even at 5 Ma. This value is considered a likely maximum age for cave systems to have opened in the Cradle of Humankind UNESCO heritage site[21,23], as suggested by the absence of older fossils in the area[17,24]. A derivation – even from a few metres below the surface (which would allow a [26]Al/[10]Be ratio range down to ~4.5) – is impossible for sample M2CA, because the absolute [10]Be abundance several million years ago would then be much lower. This mismatch suggests that the centre values for *PI* as derived from the isochron regression are inaccurate.

If M2CA is back-corrected using the parameters for *calc2* (i.e. a surface erosion rate of 5 m/Ma), the problem of its previous burial history is solved. A marginal match with near-surface abundances is achieved upward of 4.6 Ma (grey symbols and line in Figure 1b) and there is a good fit with an initial burial age of ca 5 Ma. The [10]Be and [26]Al concentrations of *calc2* correspond to the approximate upper limit for effective in-situ production rates that can provide a realistic back-correction for this sample. This result also indicates that a cave system existed at the Sterkfontein locality as early as ca 5 Ma ago, and that material reworked from this system was ultimately deposited in the Silberberg Grotto.

As the three chert samples (M2CA, M2CB and M2CC) were taken close to each other[1] (and to StW573), the same in-situ [10]Be and [26]Al production rates must have applied to all three after the sediments encasing the fossil were deposited. Using the parameters for *calc2* to

examine the past of the other chert samples is, therefore, a realistic approach. Sample M2CB yields an upper age limit for the deposit that has implications for the maximum age of StW573. In Figure 1c, the back-corrected [10]Be and [26]Al concentrations for this sample are shown together with the surface production curve. [26]Al/[10]Be ratios cannot plot above this curve (the 'forbidden zone'). The back-corrected values for M2CB using *calc2* production rates cross this limiting curve at 2.5 Ma, and lie within the forbidden zone outside 2σ (95% confidence) limits for ages over 2.8 Ma (grey symbols in Figure 1c). Values for 3.6 Ma clearly lie far in the forbidden zone. Sample M2CC is uninformative: it plots so close to the in-situ values that, in back-correcting, its error limits expand to include all possibilities. Values for the composite chert sample STM2-light cross the surface production curve at 3.2 Ma and move beyond 2σ uncertainty limits at 3.6 Ma (grey symbols in Figure 1d). While these values for STM2-light seem less restrictive, it must be noted that this sample is a composite and probably heterogeneous, so components of it would likely yield lower maximum ages than its bulk. Because StW573 was deposited in the Silberg Grotto as an articulated skeleton[13], the individual either died in situ or not long before deposition. This places a maximum age constraint of ca 2.8 Ma on the fossil. The use of 95% confidence limits boosts confidence in this result.

With the recent advances in precision and accuracy of measurements of low concentrations of [10]Be and [26]Al in quartz[1] as well as a firmer basis for calculating their production rates at depth[15], the approach taken here holds promise to be useful for reconstructing the geological history of cave systems.

Exploring a two-stage burial scenario

The maximum age for the breccia deposit encasing StW573, as determined above, appears to contradict the burial isochron date of Granger et al.[1], even if the uncertainty of the latter was underestimated through the use of composite samples. This problem may be resolved by proposing that this breccia deposit contains material that was earlier buried in a chamber at a higher level in the cave system, i.e. it is a secondary deposit. An example of such a secondary deposit in Sterkfontein Cave occurs in the Name Chamber, which contains material from Member 5 (mainly) and Member 4, derived from former higher cave levels now exposed in the open excavation.[25,26] As discussed above, the breccia surrounding StW573 contains chert fragments that are derived from various levels in the cave, going back as far as about 5 Ma, indicating that these sediments were reworked. A present-day example in the Cradle of Humankind of such a two-level cave (with a potential death trap) is Gladysvale.[27]

The deposits of Member 4 and 5, now exposed in the surface excavation pit, accumulated in a cave chamber between ca 2.5 and 1.4 Ma.[17] This chamber was de-roofed as a result of erosion, estimated at a rate of ca 5 m/Ma,[1] (rendering the land surface about 14 m higher at 2.8 Ma than today), and roof collapse. Figure 2a shows the position of this chamber (approximately delineated by the extent of the current excavation pit) relative to the Silberg Grotto. Immediately south of the open excavation a large block of dolomite occurs that shows a dip of ca 30° S (Figure 2b), while the strata at Sterkfontein generally dip 25–30° NNW. This block lies above the east end of the Silberg Grotto (Figure 2a) where the apex of its sediment cone is located.[11] It was noted by Robinson[25] as 'collapsed dolomite' but received no attention after that. This block is most likely part of a cave roof that collapsed into a void, thus documenting that a cave chamber once existed above the present Silberg Grotto. The evidence does not allow determination of whether this chamber formed part of the large cave holding Members 4, 5 and 6, or was separate from it; but the second possibility cannot be excluded.

However, whilst a two-staged burial scenario is thus not inconsistent with the geological evidence, it must be assessed whether such a scenario could possibly result in a cosmogenic isotope array resembling an isochron. To do so, we calculated the [10]Be and [26]Al concentration data of individual samples back in time, as done for the chert samples. In Figure 3, the black symbols (here with 2σ, i.e. 95% confidence, error ellipses) and solid curves show the back-correction to 2.8 Ma for sediment samples and STM2-light, calculated using Equation 2

and applying present day in-situ abundances corresponding to *calc2* of Figure 1a. Sample ST7 of Granger et al.[1], taken at the surface and indicating an erosion rate of 5–6 m/Ma, is shown for comparison.

Although STM2-light is a composite sample, its average [26]Al and [10]Be concentrations at 2.8 Ma provide the best estimate of what in-situ accumulated cosmogenic nuclide abundances in such a previous higher level cave system could have been; at 2.8 Ma they plot just below the surface production curve (Figure 3). Long-term accumulation of [26]Al and [10]Be under shielding and with a low erosion rate (as indicated by ST7) must lead to a lower [26]Al/[10]Be ratio in the sample than at the surface, as a result of the more rapid decay of [26]Al compared to [10]Be. Shielding could have many physical forms, such as overburden, or a position in a cave with a small opening. Notwithstanding the lack of constraints on actual cave configurations, cosmogenic nuclide accumulation under shielding conditions can be estimated. Various scenarios based on surface production data of Granger et al.[1], with material residing in a covered position experiencing a shielding factor that decreases from ca 99% to ca 95% over a period of ca 2 Ma, can yield [26]Al and [10]Be concentrations similar to those of 'STM2-light at 2.8 Ma' in Figure 3. This is in accord with the assessment of Granger et al.[1] that STM2-light constitutes chert debris from a higher level in the cave system. As it occurs thoroughly intermingled with material originally derived from the surface (samples ST1 and ST2), it is reasonable to conclude that the latter could also have resided at this higher level in the cave system.

Before first burial, all surface-derived samples must have had [10]Be and [26]Al concentrations plotting on the surface production curve. Given the rather large 2σ uncertainties of the back-corrected concentrations at 2.8 Ma for most samples, most of the additional correction times calculated to bring each sample back to the surface production curve also have large uncertainties. This can be illustrated by considering the varying distances from individual error ellipses to the surface production curve. For each surface-derived sample, the minimum correction time needed to intersect the surface production curve is estimated by back-correcting the point on its error ellipse closest to the surface production curve beyond 2.8 Ma, using Equation 2 (grey dot–dash curves and symbols in Figure 3). The production values corresponding to in-situ [10]Be and [26]Al steady-state concentrations of 'STM2-light at 2.8 Ma' were used for this as a best estimate. The correction times are listed for each sample in Figure 3. In a two-stage burial model, these represent the minimum residence times in the upper chamber before the samples were redeposited into their current position. It can be seen that the minimum residence times vary from 0 to 0.5 Ma (in a similar manner the maximum potential residence times can be calculated, which for all samples are >1 Ma). Note that the heterogeneity of the samples is highlighted by the surface curve intersection for composite sample STM2-dark, which reflects a higher apparent erosion rate (shorter surface residence time) than any of the bulk samples from which it was derived, indicating that the individual samples are mixtures of grain populations with different surface residence times. Interestingly, all apparent minimum pre-burial erosion rates are much lower than the erosion rate measured for today using sample ST7.[1] This difference may reflect either lower true erosion rates[21,28] or higher chemical erosion factors[29] in the past, with more of the dolomite being removed by dissolution at the surface as a consequence of a more humid climate[30].

This analysis demonstrates that an apparent isochron age of 3.67±0.16 Ma can be obtained for a secondary deposit which was laid down at a much younger age (2.8 Ma in our example), but which reworked surface-derived material that had accumulated in an upper chamber over a period as long as 1 Ma (2.8–3.8 Ma) or possibly even longer. At the same time, this observation points to a way of testing the two-staged burial hypothesis. The data array of Granger et al.[1] is technically an isochron (meaning that any scatter of the data can be the result of analytical uncertainty) because of the rather large error limits of the data on the surface-derived samples. As shown by the chert data, it should now be possible to obtain greater precision for surface-derived samples as well. If an array with greater precision on the data from surface-derived samples (and no composites) still qualifies as an isochron, then the two-staged burial hypothesis is incorrect. If there is significant scatter, it is correct.
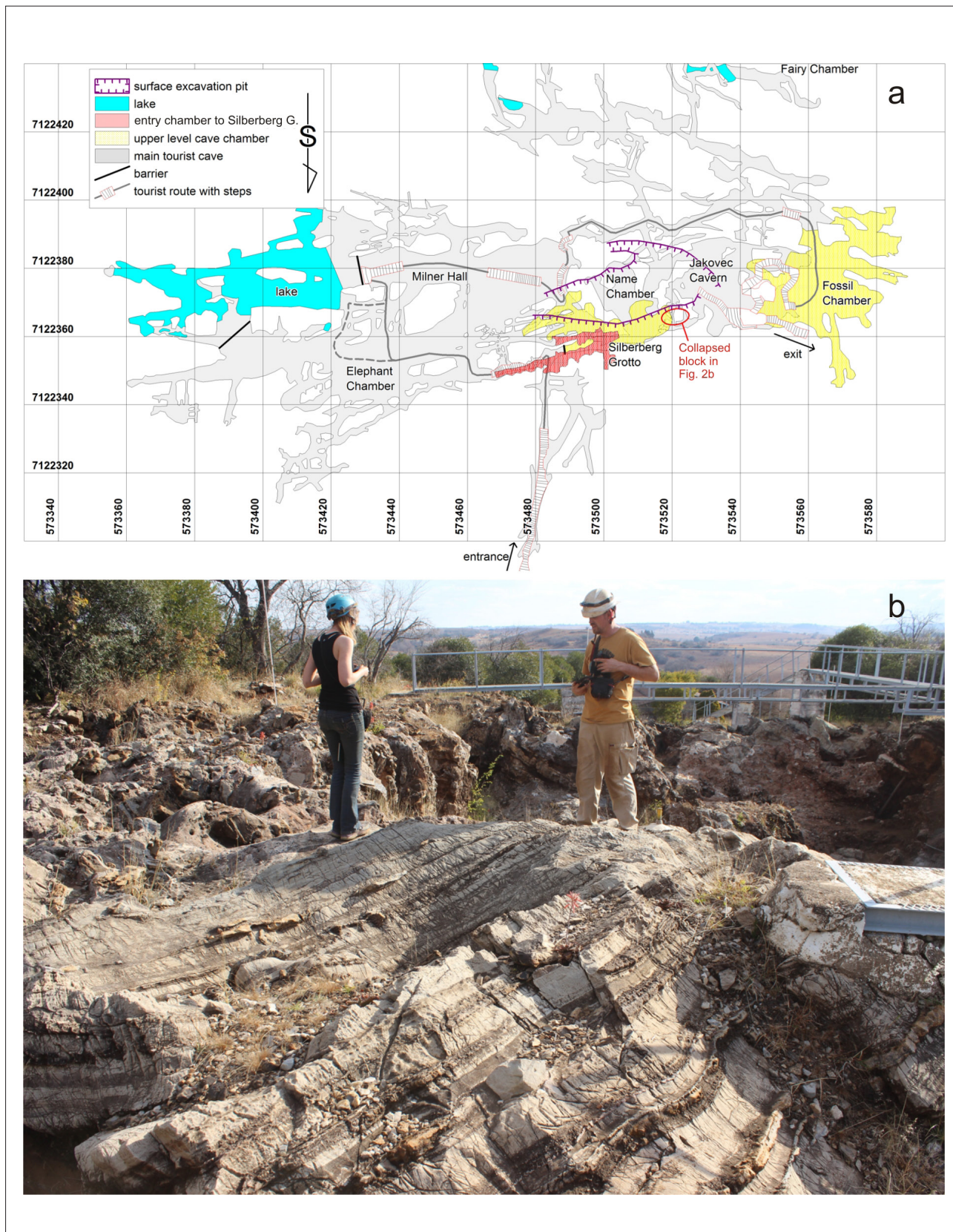
(a) Source: Adapted from Martini et al.[41]; (b) Photo: Paul Dirks

Figure 2: Prominent surface feature at Sterkfontein and its relation to the Silberberg Grotto. (a) Cave map showing the position of surface workings, entry chambers and (b) relative to the Silberberg Grotto. (b) View from the east of a large tilted dolomite block on the south side of the open excavation, adjoining breccia of Member 4.
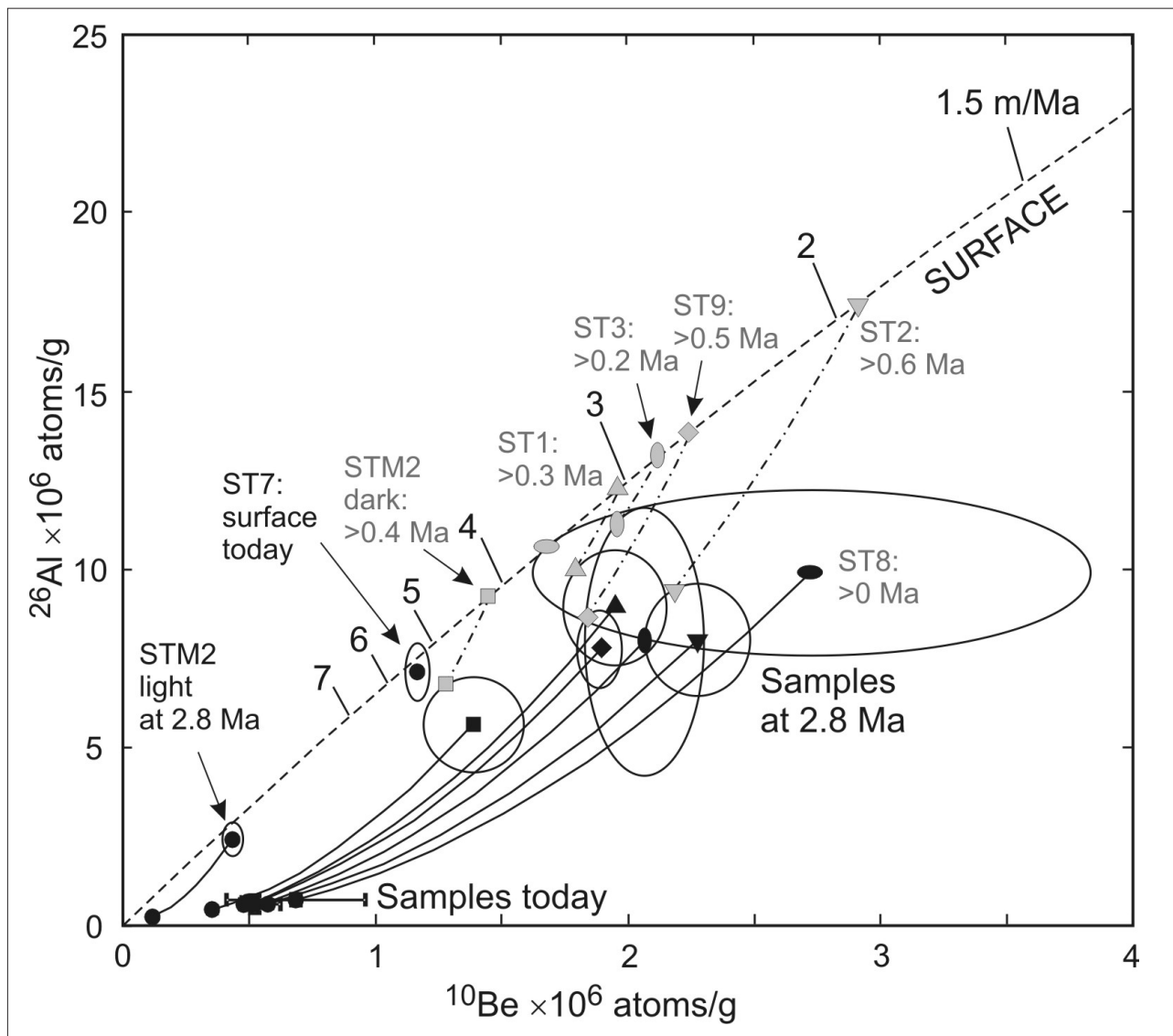
Figure 3: Back-correction of sample data in a two-stage burial model. Black symbols and solid curves show back-corrected decay paths of surface-derived samples and chert composite 'STM2-light' to 2.8 Ma, calculated using Equation 2 and in-situ ^{10}Be and ^{26}Al production rates corresponding to '*calc2*' values of Figure 1a. Error ellipses show 2σ uncertainties, derived from Granger et al.[1] Data for ST7 (present-day surface sample of Granger et al.[1]) is shown for comparison. Dashed curve 'SURFACE' shows surface steady-state ^{10}Be and ^{26}Al concentrations for a range of erosion rates. Grey dot–dash curves are decay paths in a hypothetical upper cave chamber, calculated back to their pre-burial values at surface, using in-situ ^{10}Be and ^{26}Al production rates corresponding to the concentrations of 'STM2-light at 2.8 Ma'. Minimum times required to correct back to surface values, given for each sample, yield minimum residence times in the upper chamber. Note the error ellipse for sample ST8 touches the surface curve: minimum residence time is zero for this sample.

Discussion

While we have shown that the isochron of Granger et al.[1] can be compatible with a two-stage burial scenario, the question remains as to how fossil StW573 could be younger than 2.8 million years old and be embedded in sediments that have been underground for (on average) over 3.5 Ma. In assessing possible models that fulfil the constraints imposed by the cosmogenic isotopes, our interpretation must also be consistent with the broader faunal content of sediments in the Silberberg Grotto, and palaeomagnetic results obtained from the flowstones within them (whether intrusive or stratigraphic).

To reconstruct plausible burial scenarios for StW573, it is important to assess the facies associations of the sediments surrounding the fossil, as described by Bruxelles et al.[10] These sediments are composed of surface-derived rubble, sand and mud as well as dolomite and chert fragments of varying sizes that are thoroughly mixed together.[1,10] The deposits occur as a series of layers that consist of matrix-supported breccia in which angular chert and dolomite blocks are embedded in a muddy, fine- to coarse-grained sandstone matrix with no internal structure. The clasts display a degree of grading, with variable clast sizes and clast densities across layers. The clastic sequence displays no evidence of suspension flow (e.g. cross-bedding, matrix grading, erosional channels) or standing water (e.g. mud drapes), although shelf stones show that the grotto was filled with water at times after its deposition.[11]

The deposits around StW573 have been described as the proximal to medial part of a talus cone.[11,31] The sedimentary features summarised above are consistent with the deposits being a series of sheet-like debris flows, i.e. mixtures of water, mud, sand and breccia blocks with the internal strength and ability to carry blocks (and bodies) in the matrix[32,33], yet producing preferred orientation of clasts[34]. These debris flows would have moved down the slope of a talus cone from an entry point, presumably within the roof to the eastern corner of the Silberberg Grotto.[11] The debris flow deposits display variable composition, reflecting variations in water content, provenance sediment and flow rates, but each layer was probably deposited rapidly, as demonstrated by Unit B2b[10], which

envelops the fully articulated skeleton of StW573 and preserves complex body configurations of otherwise delicate elements, such as the clasped hand[13]. The rate of accumulation of the sequence as a whole cannot be determined from the sedimentology, and the isochron, being 'un-sharp', cannot constrain this aspect with any degree of confidence.

The fossil assemblage in the Silberberg Grotto preferentially comprises animals with climbing proclivities (i.e. primates and carnivores), and conspicuously lacks evidence of predator damage.[11,17] The taphonomic data indicate that many faunal remains are from individuals that entered the Silberberg Grotto on their own and were then unable to escape[35], i.e. the grotto acted as a death trap. In contrast to Member 4, which contains many hominin remains, the only hominin fossils in Member 2 are the remains of StW573, and thus the occurrence that led to a hominid entering the Silberberg Grotto appears to be rare.[35] Fossil StW573 lies embedded in Unit B2b and is thought to have been preserved in the death position,[10,13] implying that the individual died while being entombed in the debris flow, or shortly before.

When taken together, evidence suggests that StW573 ventured into an upper cave and wandered, or fell, into the Silberberg Grotto where it died and was buried. The reasons for entering the upper chamber could be many (e.g. to search for water, security, shelter), and it is plausible that the individual (like other animals in the Member 2 deposit) was unaware of the presence of the death trap, because they were unfamiliar with the cave system, or the death trap had recently formed (e.g. because part of the roof of the Silberberg Grotto had opened). Live animals falling into a death trap in such a situation can be accompanied, preceded or followed by unconsolidated sediment material that has been lying in the upper cave for hundreds of thousands of years. Erosion and re-deposition of sediment accumulations in the upper chamber would be even more likely if a passageway between the upper chamber and the Silberberg Grotto below had opened suddenly. Such a transient passageway would have disturbed the depositional environment in the upper chamber, allowing erosion, and could have created the death trap. Thus, the age for StW573 could be much younger than the cosmogenic burial age of the sediments that are now associated with the fossil in the Silberberg Grotto.

The assumption that unconsolidated sediment can be preserved in an upper chamber needs further comment. The sediment record of caves in the Cradle of Humankind site shows a significant bias towards fully lithified (i.e. calcified) sediments composed of coarser-grained, more permeable material indurated with calcite cement. In contrast, finer-grained, muddy, and less permeable material is less likely to be strongly indurated and lithified, and therefore less likely to be preserved. Yet some caves, such as the nearby Rising Star Cave[36], are known to have contained large volumes of mostly unconsolidated sediment, much of which has been eroded in response to water movement through the cave. Other examples of poorly consolidated sediment accumulations in caves include the upper flowstone-bounded units of Gladysvale with ages of up to 0.5 Ma,[27] and parts of the Member 2 deposits in the Silberberg Grotto itself (e.g. unit B2a underneath StW573[10]). Therefore, it should not come as a surprise that unconsolidated sediment may have existed for hundreds of thousands of years in an upper chamber above the Silberberg Grotto, before being washed down.

How does the burial scenario for StW573 fit with other dating constraints for sediments in the Silberberg Grotto? Palaeomagnetic work done on $CaCO_3$ units and associated siltstone material in the deposit hosting StW573 shows reverse polarity in the units below the fossil, and normal polarity at the level of the fossil and above.[37] The $CaCO_3$ units around StW573 (F2 to F4) are not flowstones, but intrusive fracture fillings.[7,10,37] According to Bruxelles et al.[10], the lower unit (F1) is also intrusive based on the presence of a void immediately above it in which botryoidal $CaCO_3$ has formed, but no real evidence is presented that F1 is not a flowstone. If the F1 unit is a stratigraphic flowstone, then the part of the deposit below StW573 would be placed in a reverse-polarity period. Given a minimum age of ca 2.2 Ma,[7,9] based on the age of the intrusive $CaCO_3$ units, and in case of a maximum age of 2.8 Ma as discussed above, the Matuyama C2r.2r Chron (2.58–2.16 Ma) would then be the only candidate.[37] If all $CaCO_3$ units are intrusive, the palaeomagnetic data have no bearing on the age of the fossil.

The fauna in the deposits of the Silberberg Grotto is largely a subset of that in Member 4 of Sterkfontein and is not highly diagnostic for age.[5,17] The fauna includes two taxa of extinct hunting hyena, *Chasmaporthetis nitidula* and *Ch. silberbergi*[38], and in the former, a similarity in primitive dentition to *Ch. australis* from the lower Pliocene fossil deposit of Langebaanweg is noted – 'although it is not clear at this stage that the two are conspecific'[38]. However, both taxa also occur in Member 4 of Sterkfontein[17], as well as in Member 1 of the Swartkrans site[24]. Member 4 has been reliably dated to between ca 2.6 Ma and 2.0 Ma by U-Pb on flowstones[7]; and at Swartkrans, $^{26}Al/^{10}Be$ burial ages from Member 1 sediments concur with U-Pb ages of flowstones between ca 2.2 and 1.8 Ma[39,40]. On the other hand, the extinct colobine monkey *Cercopithecoides williamsi*, found in the Silberberg Grotto deposits[17] as well as in Member 4 and Swartkrans Member 1[5,24], is noted as not having been reported from reliably dated sites older than 2.5 Ma[5]. In summary, no contradiction arises from these faunal data in the case of an age <2.8 Ma for the deposit encasing StW 573.

Conclusion

Cosmogenic ^{10}Be and ^{26}Al data on chert fragments from a cave deposit can impose constraints on the age of that deposit. In the case of the sediments encasing StW573, such data[1] indicate that this deposit was formed no earlier than 2.8 Ma, even if its components had been underground for (variably) longer periods, yielding an isochron age of 3.67 ± 0.16 Ma.[1] The younger age is not in conflict with faunal studies[5,17,24], palaeomagnetic work[37] and U-Pb dating[7,9]. The apparent contradiction can be resolved by invoking a two-stage burial scenario, which is geologically realistic. This scenario can ultimately yield an isochron-like data array even if primary burial ages differ among samples. It requires (1) an upper cave level environment in which sediment accumulated over time, and (2) events in which the accumulated sediment matter, including chert fragments derived from within the cave, dropped to a deeper level in the form of debris flows and was chaotically mingled. Because the fossil was incorporated as an articulated skeleton, it cannot be older than the deposit, and the individual must, therefore, have fallen into the lower cave either on its own, or incorporated in a debris flow. As the two-stage burial scenario can reconcile the indicated 2.8 Ma maximum age for the fossil with the much older isochron date, it deserves serious consideration.

Acknowledgements

Authors' contributions

J.D.K. contributed the considerations and calculations relating to cosmogenic nuclide systematics. P.H.G.M.D. contributed the sedi-mentological and taphonomical review and arguments. Both authors wrote their respective parts of the manuscript.

References

1. Granger DE, Gibbon RJ, Kuman K, Clarke RJ, Bruxelles L, Caffee MW. New cosmogenic burial ages for Sterkfontein Member 2 *Australopithecus* and Member 5 Oldowan. Nature. 2015;522:85–88. http://dx.doi.org/10.1038/nature14268

2. Clarke RJ. First ever discovery of a well-preserved skull and associated skeleton of *Australopithecus*. S Afr J Sci. 1998;94:460–463.

3. Partridge TC, Watt IB. The stratigraphy of the Sterkfontein hominid deposit and its relationship to the underground cave system. Palaeont Afr. 1991;28:35–40.

4. Partridge TC, Shaw J, Heslop D, Clarke RJ. The new hominid skeleton from Sterkfontein, South Africa: Age and preliminary assessment. J Quat Sci. 1999;14:192–198. http://dx.doi.org/10.1002/(SICI)1099-1417(199907)14:4<293::AID-JQS471>3.0.CO;2-X

5. Berger LR, Lacruz R, De Ruiter DJ. Revised age estimates of *Australopithecus*-bearing deposits at Sterkfontein, South Africa. Am J Phys Anthropol. 2002;119:192–197. http://dx.doi.org/10.1002/ajpa.10156

6. Clarke RJ. On the unrealistic 'Revised age estimates' for Sterkfontein. S Afr J Sci. 2002;98:415–418.

7. Pickering R, Kramers JD. Re-appraisal of the stratigraphy and determinations of new U-Pb dates for the Sterkfontein hominin site, South Africa. J Hum Evol. 2010;59:70–86. http://dx.doi.org/10.1016/j.jhevol.2010.03.014

8. Partridge TC, Granger DE, Caffee MW, Clarke RJ. Lower Pliocene hominid remains from Sterkfontein. Science. 2003;300:607–612. http://dx.doi.org/10.1126/science.1081651

9. Walker J, Cliff RA, Latham AG. U-Pb isotopic age of the StW 573 hominid from Sterkfontein, South Africa. Science. 2006;314:1592–1594. http://dx.doi.org/10.1126/science.1132916

10. Bruxelles L, Clarke RJ, Maire R, Ortega R, Stratford D. Stratigraphic analysis of the Sterkfontein StW 573 *Australopithecus* skeleton and implications for its age. J Hum Evol. 2014;70:36–48. http://dx.doi.org/10.1016/j.jhevol.2014.02.014

11. Clarke RJ. A deeper understanding of the stratigraphy of Sterkfontein fossil hominid site. Trans R Soc S Afr. 2006;61:111–120. http://dx.doi.org/10.1080/00359190609519960

12. Dirks PHGM, Kibii JM, Kuhn BF, Steininger C, Churchill SE, Kramers JD, et al. Geological setting and age of *Australopithecus sediba* from southern Africa. Science. 2010;328:205–208. http://dx.doi.org/10.1126/science.1184950

13. Clarke RJ. Newly revealed information on the Sterkfontein Member 2 *Australopithecus* skeleton. S Afr J Sci. 2002;98:523–526.

14. Balco G, Rovey CWII. An isochron method for cosmogenic-nuclide dating of buried soils and sediments. Am J Sci. 2008;308:1083–1114. http://dx.doi.org/10.2475/10.2008.02

15. Balco G, Soreghan GS, Sweet DE, Marra KR, Bierman PR. Cosmogenic-nuclide burial ages for Pleistocene sedimentary fill in Unaweep Canyon, Colorado, USA. Quat Geochronol. 2013;18:149–157. http://dx.doi.org/10.1016/j.quageo.2013.02.002

16. Erlanger ED, Granger DE, Gibbon RJ. Rock uplift rates in South Africa from isochron burial dating of fluvial and marine terraces. Geology. 2012;40:1019–1022. http://dx.doi.org/10.1130/G33172.1

17. Reynolds SC, Kibii JM. Sterkfontein at 75: Review of palaeoenvironments, fauna, dating and archaeology from the hominin site of Sterkfontein (Gauteng Province, South Africa). Palaeont Afr. 2011;46:59–88.

18. Lal D. Cosmic ray labeling of erosion surfaces: *In situ* nuclide production rates and erosion models. Earth Planet Sci Lett. 1991;104:424–439. http://dx.doi.org/10.1016/0012-821X(91)90220-C

19. Heisinger B, Lal D, Jull AJT, Kubik P, Ivy-Ochs S, Neumaier S, et al. Production of selected cosmogenic radionuclides by muons 1: Fast muons. Earth Planet Sci Lett. 2002;200:345–355. http://dx.doi.org/10.1016/S0012-821X(02)00640-4

20. Heisinger B, Lal D, Jull AJT, Kubik P, Ivy-Ochs S, Knie K, et al. Production of selected radionuclides by muons 2: Capture of negative muons. Earth Planet Sci Lett. 2002;200:357–369. http://dx.doi.org/10.1016/S0012-821X(02)00641-6

21. Dirks PHGM, Placzek C, Fink D, Dosseto A, Roberts EM. Using ^{10}Be dating to reconstruct the evolving landscape in the Cradle of Humankind, South Africa. J Hum Evol. 2016;96:19–34. http://dx.doi.org/10.1016/j.jhevol.2016.03.002

22. Desilets D, Zreda M. On scaling cosmogenic nuclide production rates for altitude and latitude using cosmic-ray measurements. Earth Planet Sci Lett. 2001;193:213–225. http://dx.doi.org/10.1016/S0012-821X(01)00477-0

23. Partridge TC. Geomorphological dating of cave opening at Makapansgat, Sterkfontein, Swartkrans and Taung. Nature. 1973;246:75–79. http://dx.doi.org/10.1038/246075a0

24. McKee JK. Further chronological seriations of southern African Pliocene and Pleistocene mammalian fauna assemblages. Palaeont Afr. 1995;32:11–16.

25. Robinson JT. Australopithecines and artefacts at Sterkfontein. Part One: Sterkfontein stratigraphy and the significance of the extension site. S Afr Archaeol Bull. 1962;17:87–107. http://dx.doi.org/10.2307/3886942

26. Val A, Stratford DJ. The macrovertebrate fossil assemblage from the Name Chamber, Sterkfontein: Taxonomy, taphonomy and implications for site formation processes. Palaeont Afr. 2015;50:1–17.

27. Pickering R, Hancock PJ, Lee-Thorp JA, Grün R, Mortimer GE, McCulloch M, et al. Stratigraphy, U-Th chronology, and paleoenvironments at Gladysvale Cave: Insights into the climatic control of South African hominin-bearing cave deposits. J Hum Evol. 2007;53:602–619. http://dx.doi.org/10.1016/j.jhevol.2007.02.005

28. Dirks PHGM, Berger LR. Hominin-bearing caves and landscape dynamics in the Cradle of Humankind, South Africa. J Afr Earth Sci. 2013;78:109–131. http://dx.doi.org/10.1016/j.jafrearsci.2012.09.012

29. Riebe CS, Granger DE. Quantifying effects of deep and near-surface chemical erosion on cosmogenic nuclides in soils, saprolite, and sediment. Earth Surf Process Landforms. 2013;38:523–533. http://dx.doi.org/10.1002/esp.3339

30. Bobe R, Behrensmeyer AK. The expansion of grassland ecosystems in Africa in relation to mammalian evolution and the origin of the genus *Homo*. Palaeogeogr Palaeocl. 2004;207:399–420. http://dx.doi.org/10.1016/j.palaeo.2003.09.033

31. Stratford D, Grab S, Pickering TR. The stratigraphy and formation history of fossil- and artefact-bearing sediments in the Milner Hall, Sterkfontein Cave, South Africa: New interpretations and implications for palaeoanthropology and archaeology. J Afr Earth Sci. 2014;96:155–167. http://dx.doi.org/10.1016/j.jafrearsci.2014.04.002

32. Coussot P, Meunier M. Recognition, classification and mechanical description of debris flows. Earth Sci Rev. 1996;40:209–227. http://dx.doi.org/10.1016/0012-8252(95)00065-8

33. Iverson RM. The physics of debris flows. Rev Geophys. 1997;35:245–296. http://dx.doi.org/10.1029/97RG00426

34. Major JJ. Pebble orientation on large, experimental debris-flow deposits. Sed Geol. 1998;117:151–164. http://dx.doi.org/10.1016/S0037-0738(98)00014-1

35. Pickering TR, Clarke RJ, Heaton JL. The context of Stw573, an early hominid skull and skeleton from Sterkfontein Member 2: Taphonomy and paleoenvironment. J Hum Evol. 2004;46:279–297. http://dx.doi.org/10.1016/j.jhevol.2003.12.001

36. Dirks PHGM, Berger LR, Roberts EM, Kramers JD, Hawks J, Randolph-Quinney PS, et al. Geological and taphonomic context for the new hominin species *Homo naledi* from the Dinaledi Chamber, South Africa. eLIFE. 2015;4, Art. e09561, 37 pages. http://dx.doi.org/10.7554/eLife.09561

37. Herries AIR, Shaw J. Palaeomagnetic analysis of the Sterkfontein palaeocave deposits: Implications for the age of the hominin fossils and stone tool industries. J Hum Evol. 2011; 60:523–539. http://dx.doi.org/10.1016/j.jhevol.2010.09.001

38. Turner A. Further remains of carnivore (Mammalia) from the Sterkfontein hominid site. Palaeont Afr. 1997;34:115–126.

39. Gibbon RJ, Pickering TR, Sutton MB, Heaton JL, Kuman K, Clarke RJ, et al. Cosmogenic nuclide burial dating of hominin-bearing Pleistocene cave deposits at Swartkrans, South Africa. Quat Geochron. 2014;24:10–15. http://dx.doi.org/10.1016/j.quageo.2014.07.004

40. Pickering R, Kramers JD, Hancox PJ, De Ruiter DJ, Woodhead JD. Contemporary flowstone development links early hominin bearing cave deposits in South Africa. Earth Planet Sci Lett. 2011;306:23–32. http://dx.doi.org/10.1016/j.epsl.2011.03.019

41. Martini JEJ, Wipplinger PE, Moen HFG, Keyser A. Contribution to the speleology of Sterkfontein Cave, Gauteng Province, South Africa. Int J Speleo. 2003;32:43–69. http://dx.doi.org/10.5038/1827-806X.32.1.4